

Electronic Structures of Ion Radicals of N-Heteroaromatic Hydrocarbons as Studied by ESR and Optical Spectroscopy

Tatsuhisa Kato and Tadamasa Shida*

Contribution from the Department of Chemistry, Faculty of Science, Kyoto University, Kyoto 606, Japan. Received November 20, 1978

Abstract: Various N-heterosubstituted benzenes, naphthalenes, anthracenes, and phenanthrenes have been ionized to their ion radicals in frozen solutions through intermolecular charge transfer induced by γ -ray irradiation. Cation and anion radicals have been produced selectively and studied by ESR and optical spectroscopy. The cations can be grouped into those in which the spin density is localized mainly on the in-plane lone-pair orbitals of nitrogen ("n cations") and those in which the density is distributed over a π -electron orbital (" π cations"). They can be unambiguously distinguished by ESR and optical spectra. For the n cations the optical transition energies are in accord with photoelectron spectra. The spin density of the n cations substantiates significant interactions of lone-pair orbitals as elaborated previously in terms of through-space and through-bond interactions. The π cations and π anions exhibit an approximate mirror image relation in the optical spectrum. Failure of CNDO/S calculations to account for the observed optical spectra of n cations suggests σ - π interactions.

Introduction

In studying electronic structures of molecules N-heteroaromatic hydrocarbons have been favorite examples because of the possible participation of nitrogen lone-pair electrons and of the inductive effect of aza substitution. The traditional spectroscopic work is discussed in textbooks.¹ Relatively abundant information is also available for triplet states² and anion radicals from ESR studies.³ More recently, photoelectron spectroscopy has provided direct information concerning the order of π and lone-pair ionization potentials.⁴

A survey of the literature, however, reveals a paucity of experimental data of the electronic spectra of both cation and anion radicals of the molecules and of the ESR spectra of cation radicals. Obviously, this is because the radicals are in general highly reactive and because the ionization potentials of the molecules are relatively high.

To fill this gap of knowledge a comprehensive study of the electronic structure of N-heteroaromatics has been undertaken which constitutes part of our systematic studies on ion radicals.⁵

Many N-heteroaromatic hydrocarbons, except for the prototype pyridine (vide infra), have been subjected to γ -ray irradiation in rigid glassy solutions frozen at 77 K, which has been established to induce selective ionization of the dissolved solute molecule.⁵ The ion radicals of N-heteroaromatics produced by this technique were then studied diagnostically by the combined use of ESR and optical spectra and these results were correlated with photoelectron spectra and semiempirical molecular orbital calculations.

A principal result is that a number of new σ -type in-plane cations, in which the spin density resides mostly in the nitrogen lone-pair orbitals, are produced and identified by ESR. For convenience, the cations will be designated n cations as distinct from the familiar π -type cations. Molecules which have been predicted by photoelectron spectroscopy to yield n cations as the ground-state cation radicals exhibit ESR and optical spectra consistent with the n-cation assignment. CNDO/S calculations with unadjusted parameters fail to reproduce the observed optical spectra of n cations. However, for π cations and anions a simple Longuet-Higgins and Pople type open-shell calculation gives reasonable agreement with the experimental data. The discrepancy between experiment and theory for the n cations may be taken as incentive to further studies on σ - π interactions in polyatomic cations.

Experimental Section

All the ion radicals studied were produced by γ -ray irradiation of dilute (20–40 mM) solutions of N-heteroaromatics in methyltetrahydrofuran (MTHF) and in a Freon mixture (FM), an equimolar admixture of CCl_3F and $\text{CF}_2\text{BrCF}_2\text{Br}$, at 77 and 4 K. γ -Irradiation of the frozen solution predominantly ionizes the solvent molecules, the major component of the system. In the FM system the positive charges produced migrate intermolecularly by an electronic-resonant process to a solute molecule, whereas the electrons are immobilized by dissociative attachment to the solvent molecules.⁵ In MTHF the migratory charges are stabilized by an ion-molecule reaction of MTHF.⁵ These processes ensure the selective formation of solute anions and cations via scavenging of the migratory electrons and positive charges by solute molecules in the respective solvent. Concomitantly produced neutral fragment radicals of the aliphatic solvent molecules do not interfere significantly with the optical measurement of the ion radicals of the aromatic solutes because they absorb in the shorter wavelength regions.⁵

For the ESR measurement the signal due to the fragment radicals from MTHF, such as $\cdot\text{C}_5\text{H}_9\text{O}$, superposes on the signal of solute anions. However, for the FM solutions the "background" signal due to the solvent radicals such as $\cdot\text{CCl}_2\text{F}$ and $\cdot\text{CF}_2\text{CF}_2\text{Br}$ ⁶ fortunately causes no serious interference, probably because the randomly oriented fluorine-containing radicals in the rigid solutions disperse the signal intensities over a wide range of magnetic field. The large anisotropy in the hyperfine coupling constants of the fluorine atom causes the background signal at a particular field to be obliterated by the strong signal due to solute cations.

A 3500-Ci ⁶⁰Co γ -ray source was used for irradiation. With the radiation dose given less than 1 mM out of 20–40 mM of solute molecules is ionized. The optical spectra in this work represent the difference of absorptions before and after γ -ray irradiation. Therefore they are ascribed to the absorption due to the solute ions produced with the conversion of less than a few percent. Some samples were irradiated at 4 K and measured at the same temperature and at 77 K to find the effect of possible molecular motions at 77 K upon the spectrum. ESR and optical measurements were carried out using JEOL PE and FE series spectrometers and a Cary 171 spectrophotometer. A computer program for simulation of ESR spectra in rigid solutions was coded after the work by Kasai and his co-workers.⁷

Experimental Results

1. Cations of Diazabenzenes. The ESR spectrum of 1,2-diazabenzene (pyridazine) in FM irradiated and measured at 77 K is shown in Figure 1. Measurements at 4 K gave a virtually identical spectrum. The simulated spectrum was obtained with the parameters given in Table I. FM, containing no solutes, gave the spectrum at the bottom of Figure 4. The latter

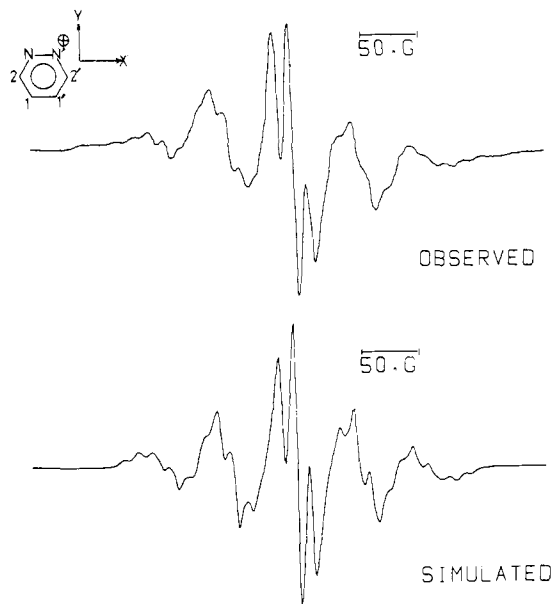


Figure 1. ESR spectra of pyridazine cation radical. Upper: observed for pyridazine in FM at 77 K. Lower: simulated with the parameters listed in Table I.

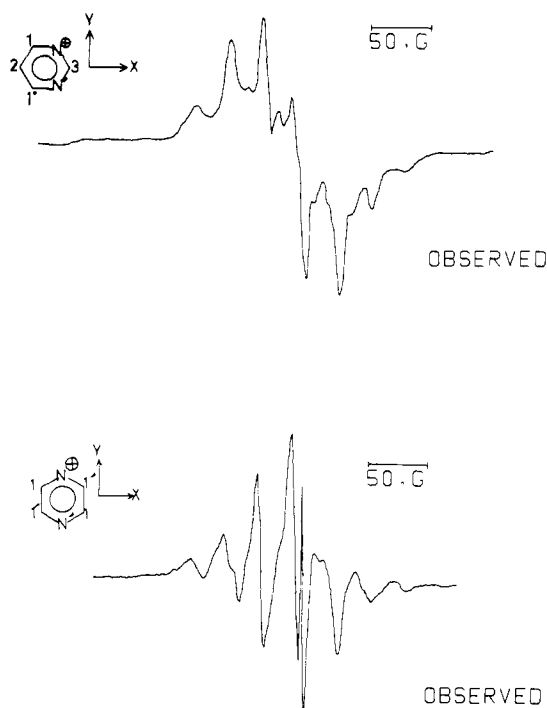


Figure 2. ESR spectra of cation radicals of pyrimidine and pyrazine in FM at 77 K.

spectrum serves as the background for all the spectra of FM solutions, the sharp singlet being due to color centers of the quartz cell and the doublet at the extremities due to hydrogen atoms produced on irradiation in the cells. ESR spectra are also observed for 1,3- and 1,4-diazabenzene in FM, shown in Figure 2. They agree with simulated spectra to a similar degree as in the case of pyridazine (not shown). The parameters used for the simulation are compiled in Table I.

The optical spectra of samples exhibiting the ESR spectra in Figures 1 and 2 are shown in Figure 3. The absorption bands with the peak maxima at 2.8, 1.9, and 1.8 eV for the cations of 1,2-, 1,3-, and 1,4-diazabenzene, respectively, are attributed

Table I. ESR Parameters of the *n* Cations as Determined from the Best-Fitting Simulation^a

Pyridazine						
g values	x	y	z	θ		
	x	y	z			
$a_{N,N'}$	50.4	68.6	51.4	$\theta_N = 4.0$	$\theta_{N'} = -4.0$	
$a_{H1,H1'}$	13.4	12.3	12.1	$\theta_{H1} = 6.8$	$\theta_{H1'} = -6.8$	
$a_{H2,H2'}$	7.6	1.3	0.3	$\theta_{H2} = 10.7$	$\theta_{H2'} = -10.7$	
Pyrimidine						
g values	x	y	z	θ		
	x	y	z			
$a_{N,N'}$	6.1	25.8	7.0	$\theta_N = 9.7$	$\theta_{N'} = -9.7$	
$a_{H1,H1'}$	29.7	26.6	26.2	$\theta_{H1} = 14.6$	$\theta_{H1'} = -14.6$	
a_{H2}	8.6	4.9	4.4	$\theta_{H2} = 0.0$		
a_{H3}	5.1	0.0	-1.5	$\theta_{H3} = 0.0$		
Pyrazine						
g values	x	y	z	θ		
	x	y	z			
$a_{N,N'}$	18.4	32.7	18.4	$\theta_N = 0.0$	$\theta_{N'} = 0.0$	
$a_{H1,H1'}$	34.0	29.2	28.6	$\theta_{H1} = 14.6$	$\theta_{H1'} = -14.6$	
Phthalazine						
g values	x	y	z	θ		
	x	y	z			
$a_{N,N'}$	52.3	70.1	53.1	$\theta_N = 4.0$	$\theta_{N'} = -4.0$	
$a_{H1,H1'}$	3.6	3.3	3.3	$\theta_{H1} = 1.1$	$\theta_{H1'} = -1.1$	
$a_{H2,H2'}$	1.3	-0.1	-0.3	$\theta_{H2} = 8.3$	$\theta_{H2'} = -8.3$	
$a_{H3,H3'}$	6.4	1.1	0.0	$\theta_{H3} = 9.6$	$\theta_{H3'} = -9.6$	
Cinnoline						
g values	x	y	z	θ		
	x	y	z			
a_{N1}	67.5	45.5	48.4	$\theta_{N1} = 6.7$		
a_{N2}	59.5	48.5	48.1	$\theta_{N2} = 1.4$		
a_{H1}	6.9	2.5	2.0	$\theta_{H1} = -7.9$		
a_{H2}	13.9	14.2	13.6	$\theta_{H2} = -12.6$		
a_{H3}	4.5	4.2	3.9	$\theta_{H3} = 0.0$		
a_{H4}	0.9	0.0	0.2	$\theta_{H4} = 1.5$		
a_{H5}	0.5	0.2	-0.1	$\theta_{H5} = 14.6$		
a_{H6}	6.6	2.4	2.7	$\theta_{H6} = 6.1$		
Quinoxaline						
g values	x	y	z	θ		
	x	y	z			
$a_{N,N'}$	29.9	14.9	15.5	$\theta_N = 0.9$	$\theta_{N'} = -0.9$	
$a_{H1,H1'}$	33.5	29.3	28.6	$\theta_{H1} = 14.0$	$\theta_{H1'} = -14.0$	
$a_{H2,H2'}$	24.3	21.7	21.5	$\theta_{H2} = 3.7$	$\theta_{H2'} = -3.7$	
$a_{H3,H3'}$	6.5	5.8	5.7	$\theta_{H3} = 1.7$	$\theta_{H3'} = -1.7$	
Benzocinnoline						
g values	x	y	z	θ		
	x	y	z			
$a_{N,N'}$	44.3	62.8	45.3	$\theta_N = 4.0$	$\theta_{N'} = -4.0$	
$a_{H1,H1'}$	4.5	3.2	3.1	$\theta_{H1} = 0.0$	$\theta_{H1'} = 0.0$	
$a_{H2,H2'}$	5.9	3.3	3.3	$\theta_{H2} = 7.5$	$\theta_{H2'} = -7.5$	
$a_{H3,H3'}$	1.4	1.0	0.9	$\theta_{H3} = 3.4$	$\theta_{H3'} = -3.4$	
$a_{H4,H4'}$	0.6	-0.1	-0.2	$\theta_{H4} = 4.4$	$\theta_{H4'} = -4.4$	

^a θ in degree represents the angle of rotation of coordinates for the principal values of hyperfine coupling constants a_N and a_H in gauss relative to the coordinate system shown in the inset. The numbering of the atoms is also shown.

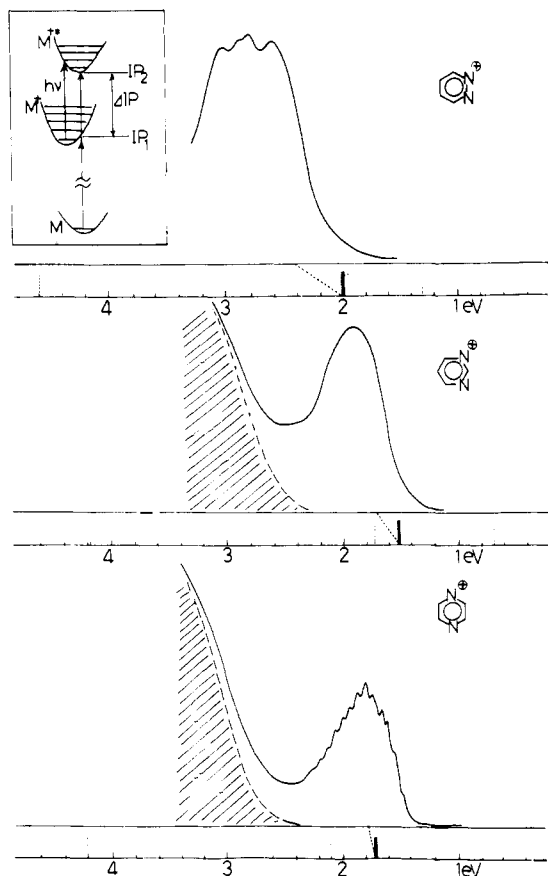


Figure 3. Optical spectra of cation radicals of diazabenzenes in FM at 77 K. The vertical bars indicate the ΔIP data of ref 8. The diagonal dotted lines indicate the correspondence between the observed optical absorption band and the symmetry-allowed $n-n$ type combination in the ΔIP diagram. The dotted bars represent the symmetry-forbidden $\pi-n$ type combinations. The inset illustrates the relation between ΔIP and the observed optical absorption $h\nu$ in terms of the schematic potential curves of a parent molecule M , cation radical in the ground state M^+ , and in the excited state M^{**} . The shaded area is regarded as due to a concomitantly produced charge-transfer complex (see text).

to the first optically allowed transitions, as will be discussed later. The hatched absorptions are attributed to a charge-transfer complex (see Discussions).

2. Cations of Monoaza- and Diazanaphthalenes. Parallel studies were extended to several naphthalene analogues. The ESR spectrum of naphthalene cation in FM shown in Figure 4 demonstrates that in the amorphous rigid solution the hyperfine structure merges into a broad singlet. 1-Aza- and 2-azanaphthalenes (quinoline and isoquinoline) gave similarly broad singlets of a peak-to-peak bandwidth of about 14–17 G. The commonly seen two weak peaks at lower fields are due to the superposing solvent radicals, as is apparent from the comparison with the bottom spectrum.

Optical spectra for quinoline and isoquinoline are shown in Figure 5. They are comparable with the spectrum of naphthalene cation.^{5c}

Dramatically different ESR and optical spectra were obtained for diazannaphthalenes as shown in Figures 6 and 7. Similarity to naphthalene cation in both ESR and optical spectra is lost. The absorption maximum at 2.15 eV of 1,2-diazannaphthalene (cinnoline), for which the photoelectron spectrum has been observed,⁸ is close to the difference of ionization energies between the two lone-pair orbitals (2.2 eV).⁸ The photoelectron spectrum of 2,3-diazannaphthalene (phthalazine) has not been reported, but the resemblance of its optical spectrum to that of cinnoline cation suggests a

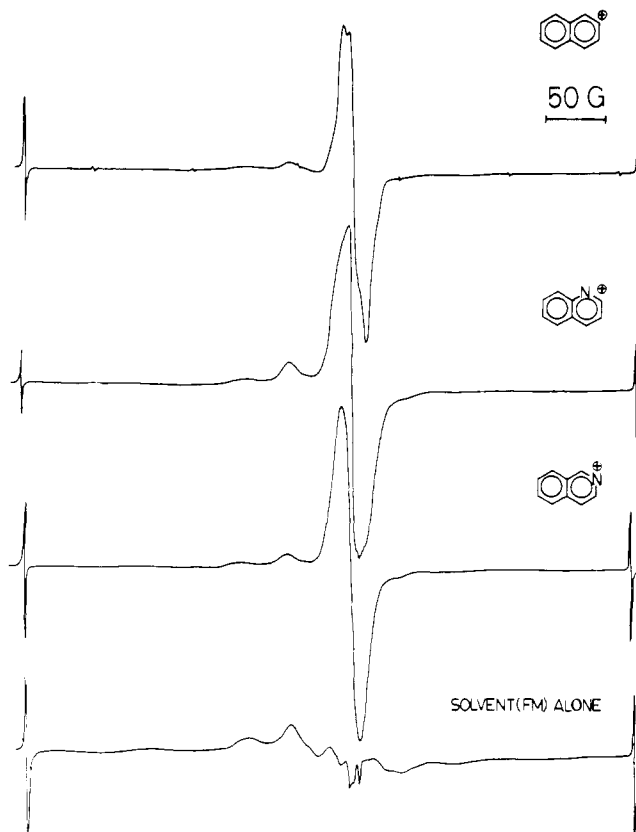


Figure 4. ESR spectra of cation radicals of naphthalene, quinoline, and isoquinoline in FM at 77 K. The bottom spectrum is for irradiated FM containing no solutes. The sharp doublet at extremities is due to hydrogen atoms, the separation being about 507 G. The small signals in the naphthalene spectrum are due to manganese ions inserted as an internal standard for magnetic field.

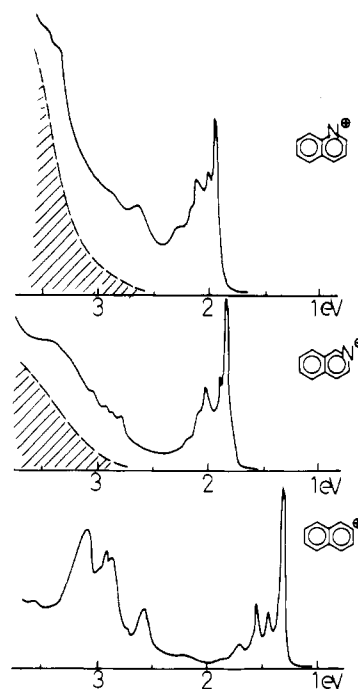


Figure 5. Optical spectra of cation radicals of quinoline, isoquinoline, and naphthalene^{5c} in FM at 77 K. The shaded area is ascribed to a charge-transfer complex as in Figure 3.

similar nature of the optical transition. Reference to the photoelectron spectrum suggests that 1,4-diazannaphthalene (quinoxaline) yields a π cation.⁸ However, the ESR and optical

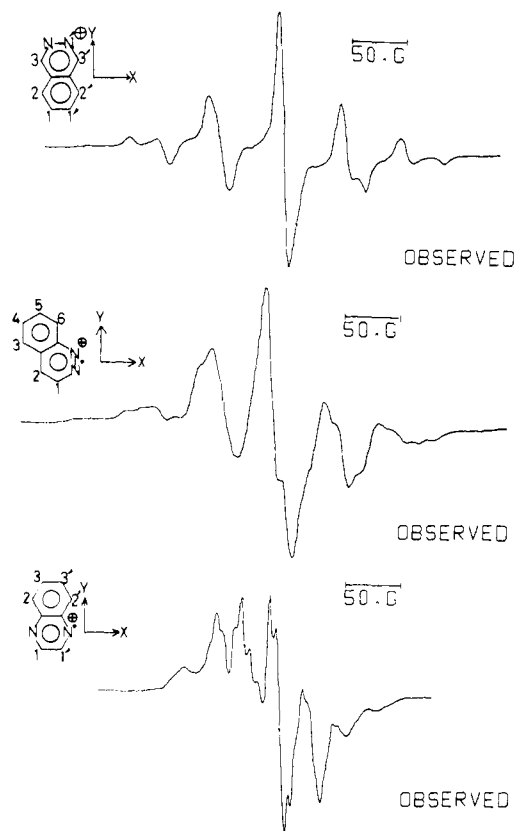


Figure 6. ESR spectra of cation radicals of phthalazine, cinnoline, and quinoxaline in FM at 77 K.

spectra are similar to those of pyrazine cation, which will be shown to be an n cation (see Discussions). The vibrational structure of the optical spectrum in Figure 7 is also reminiscent of the spectrum of pyrazine cation in Figure 3. The parameters used for the ESR simulation, listed in Table 1, indicate a large spin density localized on the nitrogen atoms, suggesting that the cations of diazaphthalenes are n type.

3. Cations of Anthracene and Phenanthrene Analogues.

Figures 8 and 9 demonstrate the optical spectra of anthracene and phenanthrene analogues irradiated in FM at 77 K. Strong similarity of the spectra to those of the cations of anthracene and phenanthrene^{3c} indicates that the cations are of π type. The schematic spectra represent the difference in photoelectron ionization potentials observed by Hush et al.⁹ The bars correspond to Hush's $\pi_2 \rightarrow \pi_1$, $\pi_3 \rightarrow \pi_1$, $\pi_4 \rightarrow \pi_1$, and $\pi_5 \rightarrow \pi_1$. The correspondence between these bars and the optical absorption bands is indicated by the dotted connecting lines.

Contrastingly, however, vicinally disubstituted 9,10-diazaphenanthrene (benzocinnoline) exhibited ESR and optical spectra indicative of the formation of n cation (Figure 10). The observed single broad band with the absorption maximum at 2.7 eV is comparable with the ΔIP value of 2.55 eV for the ionizations from the lone-pair orbitals.⁹

4. Anions of N-Heteroaromatic Hydrocarbons. A large number of anions of N-heteroaromatic hydrocarbons in fluid solutions have been studied by ESR and a tabulation for isotropic coupling constants is available.³ All the substances studied in this work were subjected to γ irradiation in MTHF at 77 K, which is known to form the respective anion radicals.⁵ The ESR spectra of the irradiated frozen solutions exhibited signals of the anion radicals consistent with the published data.³

Optical spectra of the anions have been only scatteredly reported. In the present work comprehensive optical spectra are obtained for the anions. Although spectra of some anions

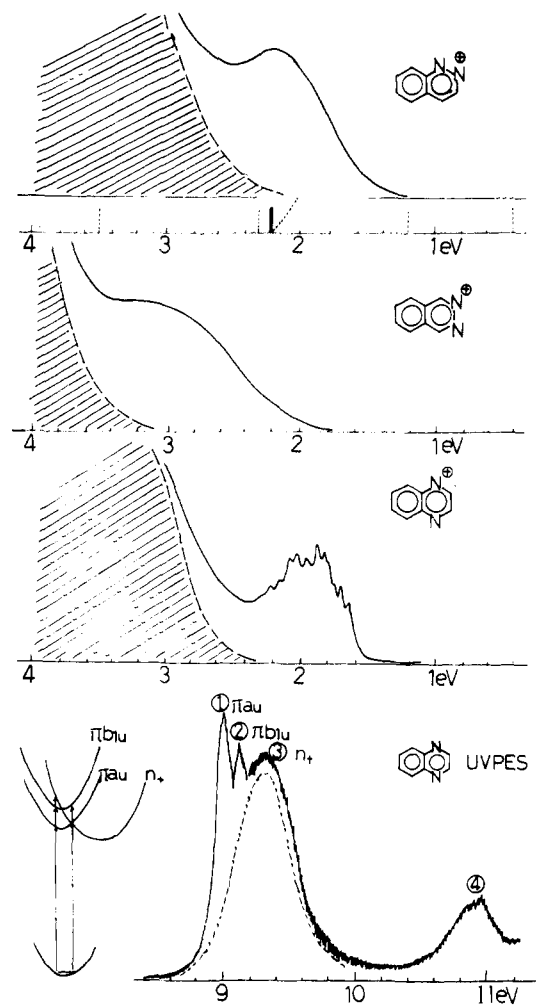


Figure 7. Optical spectra of cation radicals of diazaphthalenes in FM at 77 K. See caption for Figure 3. The UV photoelectron spectrum at the bottom is reproduced from ref 8 to show that the order of the peak maxima in UV PES may not be necessarily the same as the order of the adiabatically stable cationic states (potential minima in the scheme at the bottom left).

in Figures 11–14 are reported elsewhere (see captions for the references), the spectral range in the present work is wider and absolute intensities are given.

Discussions

Salient features of the results are summarized as follows.

(1) Cations can be divided into two groups. The first includes diaza-substituted benzenes and naphthalenes as well as vicinally diaza-substituted benzocinnoline. They are ascribed to n cations having large spin densities on the nitrogen atoms. The optical absorption bands in the visible to near-IR regions are consistent with the assignment. The transition energies of the bands are closely related to the differences of ionization energies (ΔIP) from lone-pair molecular orbitals, $n_+ = (1/\sqrt{2})(n_a + n_b)$ and $n_- = (1/\sqrt{2})(n_a - n_b)$, which have been studied in photoelectron spectroscopy.⁸ For example, the ΔIP values indicated by the vertical bars in Figures 3 and 7 correspond fairly well with the observed optical absorption bands, as in the cases discussed in a previous paper.¹¹

(2) The second group, ascribed to π cations, comprises monoazasubstituted naphthalenes and analogues of anthracene and phenanthrene except for benzocinnoline. They give ESR spectra having relatively sharp singlets and optical spectra similar to those of π cations of parent aromatic hydrocarbons.

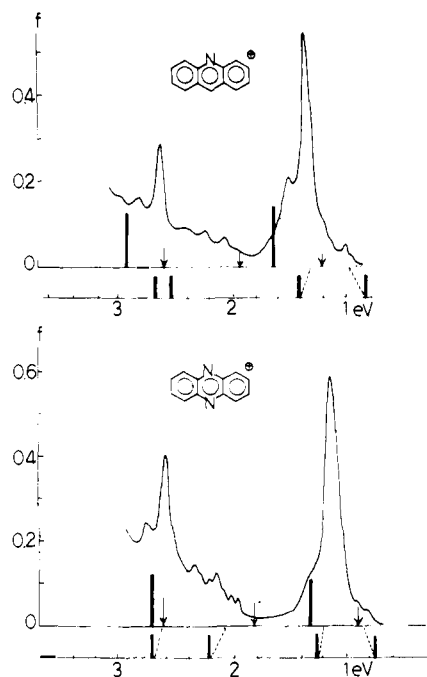


Figure 8. Optical spectra of cation radicals of acridine and phenazine in FM at 77 K. The upper set of bar spectra are obtained by a Longuet-Higgins and Pople type calculation, the value of f representing calculated oscillator strengths. The lower set of schematic spectra is constructed from the photoelectron spectra of ref 9. The bars stand for, from the right, $\pi_2-\pi_1$, $\pi_3-\pi_1$, $\pi_4-\pi_1$, and $\pi_5-\pi_1$ of Hush's assignment. The diagonal dotted lines indicate the correspondence.

(3) Anions of all the molecules studied yield optical spectra similar to those of the π anions of corresponding hydrocarbons.

There has been no report of σ cations of N-heteroaromatics, probably because they are reactive, like the isoelectronic phenyl-type hydrocarbon radicals. However, the present work shows that the cations can be produced stably in frozen media by indirect ionization through intermolecular charge migra-

tion. A standard INDO-UHF calculation yielded reasonable isotropic hyperfine coupling constants. To refine the ESR parameters, simulation was attempted. Since the spectra were observed for rigid solutions, the principal values of the anisotropic hyperfine coupling constants and of the g factors were also needed. The initial guesses of the former were calculated from the relation of McConnell and Strathdee¹² in combination with the INDO MOs. The latter were obtained by using the coefficients of the MOs and the observed ionization potentials⁸ instead of the calculated orbital energies. Repeated simulations started from the initial guesses gave such spectra as shown in Figure 1. The result of all other cases is compiled in Table I. The fact that the spin densities are delocalized over two nitrogen atoms irrespective of their separation substantiates the through-space and through-bond interactions of lone-pair electrons explored by Hoffmann et al.¹³ Attempts to account for the optical spectra of n cations by CNDO/S were unsuccessful since the calculation predicted the half-occupied orbital to be of π type and the lone-pair orbitals to be much lower in energy for most of the n cations. In view of the recent analyses of electronic structures of pyridine¹⁴ and pyrimidine¹⁵ the failure of CNDO/S is not unreasonable. Theories that can account for $\sigma-\pi$ interactions in excited large molecules are called for.

The small difference between the Δ I.P. and the transition energy, measured as the absorption maximum, may be attributed to the displacement of equilibrium configurations between the two ionic states, as indicated in the inset of Figure 3. In this connection a discrepancy between Heilbronner's and our assignments for quinoxaline should be pointed out. In their work the first ionization is assigned to be of π type from the line-profile analysis as well as from HMO calculation. In quinoxaline, however, the first few π and n orbitals lie within only 0.5 eV, as demonstrated at the bottom of Figure 7. A possible reconciliation is that their assignment is based on the vertical ionization potentials but the onset of the broad peak assigned to the ionization of the first lone-pair orbital underlies the first π peak. The scheme for Heilbronner's spectra, shown in Figure 7, indicates that the cations produced vertically in the gas phase may relax to assume the n -cation configuration in the condensed phase.

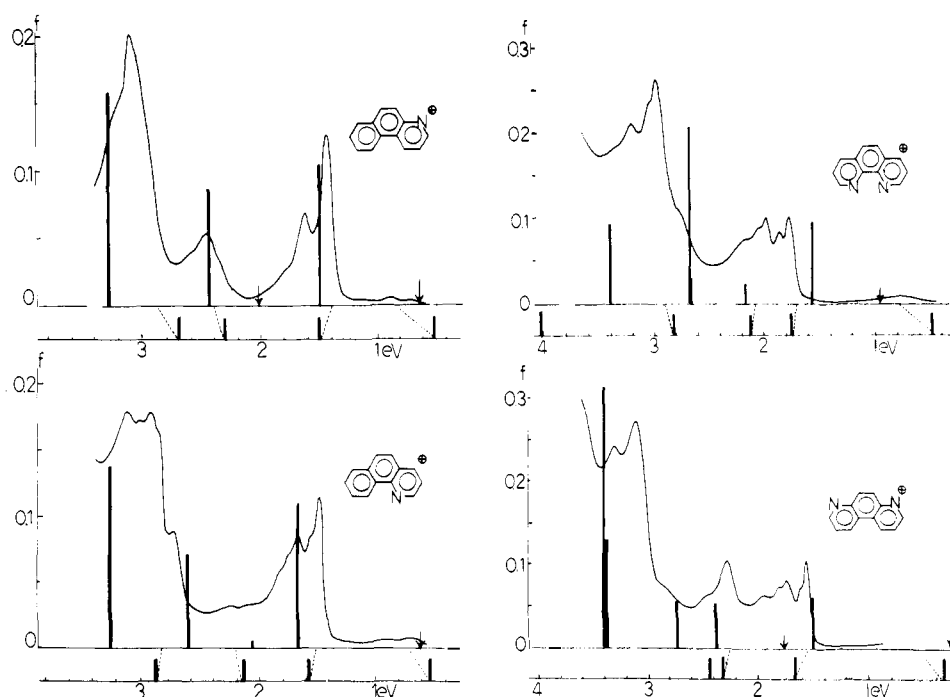


Figure 9. Optical spectra of cation radicals of phenanthrene analogues in FM at 77 K. See caption for Figure 8.

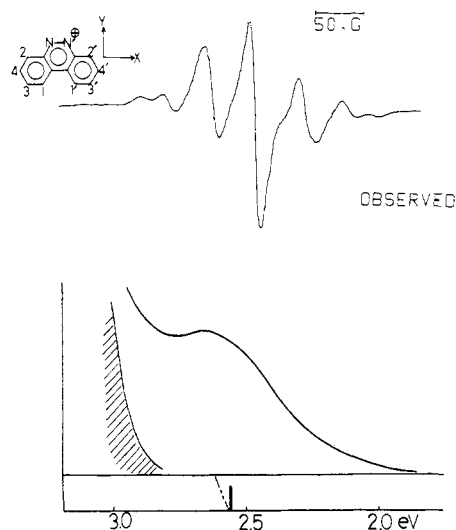


Figure 10. ESR and optical spectra of cation radical of benzocinnoline in FM at 77 K. See caption for Figure 3.

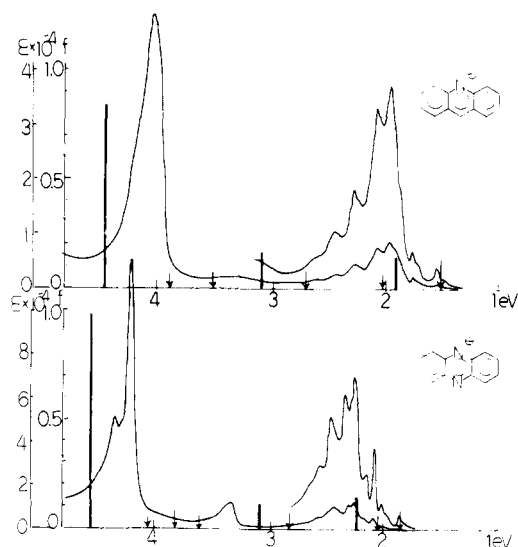


Figure 12. Optical spectra of anion radicals of azanaphthalenes in MTHF at 77 K. Crude spectra have been reported in ref 21 and 22.

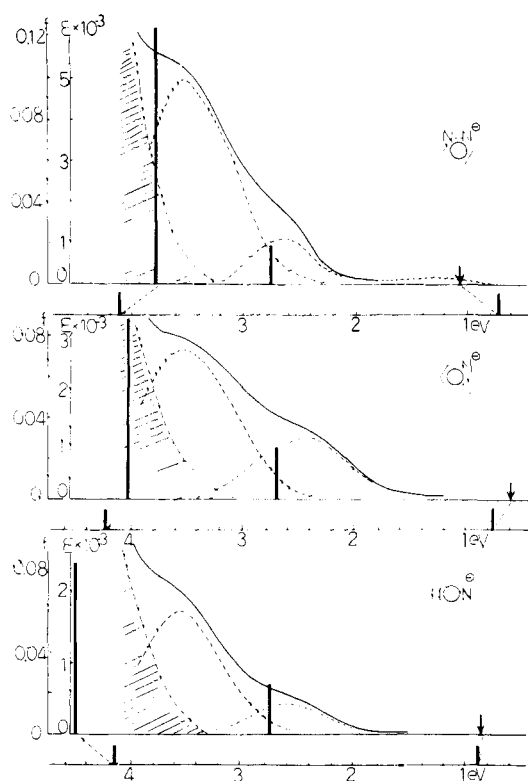


Figure 11. Optical spectra of anion radicals of diazabenzene derivatives in MTHF at 77 K. The solid observed curves are tentatively decomposed into components in broken curves. The upper schematic spectra are the result of a Longuet-Higgins and Pople type calculation. The lower schematic spectra are drawn referring to the result of ref 19.

The absorption spectra of pyrazine and quinoxaline cations (Figures 3 and 7) exhibit a long vibrational progression. A rule-of-thumb estimation of the frequency of the mode suggests that the vibration is mainly characterized by a symmetric stretching of the pyrazine framework.¹⁶

The nature of the hatched absorptions in Figures 3, 5, and 7 remains unexplained. The absorptions cannot be attributed to the *n* cations of solutes exhibiting absorptions at longer wavelengths because (1) upon limited warming of the irradiated samples from 77 K to, say, 100 K the absorption of *n* cations at longer wavelengths decayed faster than the ab-

sorption at shorter wavelengths; (2) the hatched absorptions appear to have nothing to do with the ΔIP diagram, contrary to the high correlation of the absorption assigned to the *n* cations; (3) the hatched absorptions differ from one solute to the other, therefore they cannot be due to one and the same species originating from the solvent alone. They are tentatively assigned to a charge-transfer complex involving both solute molecules and oxidizing solvent positive holes; if solutes are absent in the system, the positive hole becomes eventually a solvent-trapped positive hole which gives a known absorption with the maximum at 560 nm.¹⁷ Since this absorption is not observed at all for any of the solutions of FM, it is certain that all the migratory positive holes had reached solute molecules. Depending on the solute it may be that only part of the holes were successful in oxidizing the solute molecules to yield the cation radicals. The rest may result merely in the assumed charge-transfer complex which does not exhibit any discernible ESR spectra, probably because the spin densities are mostly localized on the side of the fluorine-containing solvent molecules complexed with the solute molecule. It must be admitted that this is a "dirty" aspect of the FM matrix, and judicious judgments are required to find the spectrum of genuine solute cations. Comparison with MO calculations as well as with photoelectron spectroscopic data should be helpful in this respect. In this context pyridine in FM is deceptive. The observation of pyridine cation radical has been problematic.¹⁸ Simpson et al. reported that γ irradiation of pyridine in FM at 77 K gave an absorption of λ_{max} 390 nm which we confirmed, but we also found that the ESR spectrum of the sample was the same as that of irradiated pure FM (Figure 4). The result indicates that pyridine is not oxidized to its cation radical by the migrating solvent positive hole. Thus, the assignment of the absorption of λ_{max} 390 nm to the cation radical seems inappropriate. We tentatively regard the absorption as being due to similar charge-transfer complexes to those discussed above.

Figures 11-14 are demonstrated for the sake of general spectral information of the rather elusive species. Among the anions, those in Figure 11 have been studied in the gas phase by electron transmission spectroscopy.¹⁹ In this spectroscopy resonances occur for anions in the ground and electronically excited states. The difference in the resonance peaks relative to the first peak corresponding to the ground-state anions is a guide for the electronic transition energies of the anions. The differences obtained from the spectroscopy predict transitions at 0.7 and 4.1 eV for pyridazine, 0.8 and 4.2 eV for pyrimidine,

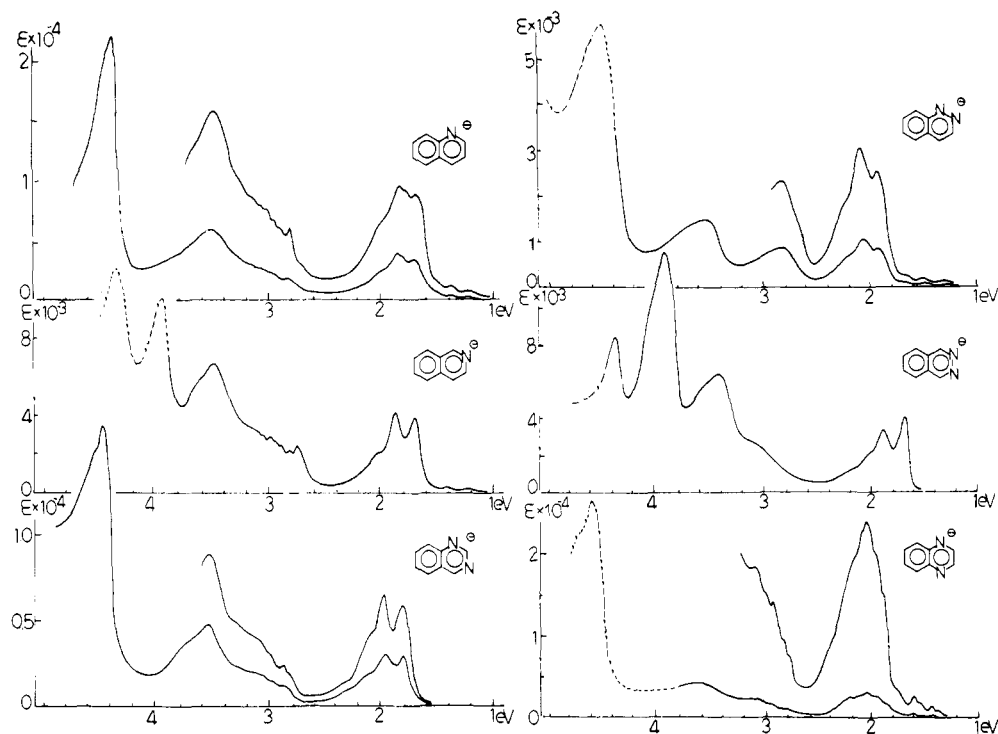


Figure 13. Optical spectra of anion radicals of anthracene analogues in MTHF at 77 K. See caption for Figure 12.

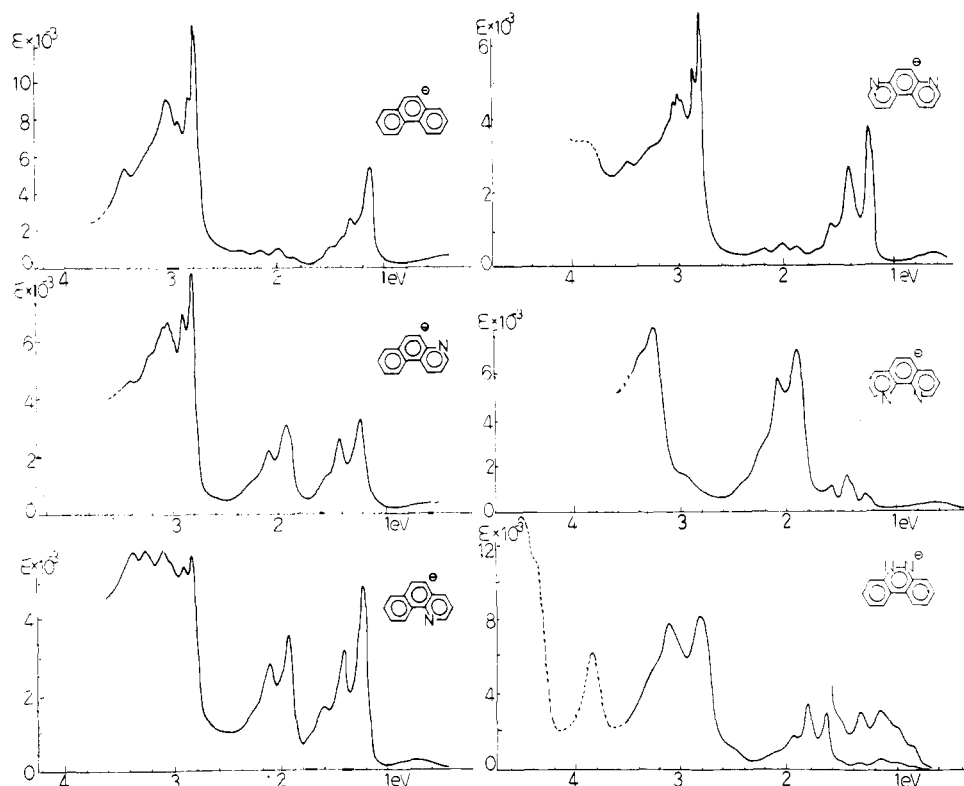


Figure 14. Optical spectra of anion radicals of phenanthrene and its analogues in MTHF at 77 K. See caption for Figure 12.

and 0.9 and 4.2 eV for pyrazine. The optical absorption spectra observed in the present work may be tentatively resolved into two broad bands as the broken curves indicate if the hatched absorptions ascribable to solvent radicals¹⁰ are ignored. The semiempirical Longuet-Higgins and Pople type calculations predict three $\pi-\pi^*$ transitions in the region of less than 4.5 eV for all anions, as the bar spectra demonstrate. The first one in the near IR should not be detectable because of the vanishing

oscillator strengths. The resolved bands are fairly close to the second and the third transitions predicted by the MO calculation whereas the first and the third transitions of the MO calculation seem to correspond to the transitions observed in the electron transmission spectroscopy designated $\bar{A} \leftarrow \bar{X}$ and $\bar{B} \leftarrow \bar{X}$ in ref 19. Since Nenner and Schulz do not show the energy region between 2 and 4 eV, it is not certain whether the resonances corresponding to the second optical transition in

Figure 11 are detectable in electron transmission spectroscopy. However, the proximity of the observed optical absorption bands at about 3.5 eV to the $\bar{B} \leftarrow \bar{X}$ transitions seems to indicate a correspondence. The broadness of the resolved bands in Figure 11 is reminiscent of a similar bandshape of benzene anion and recalls the ease of the electron detachment of optically excited anions.^{5c,20}

Note Added in Proof. The cation radical of pyridine has been recently identified to be a σ cation (see Shida, T.; Kato, T. *Chem. Phys. Lett.*, in press).

Acknowledgments. The authors wish to thank Dr. Masashi Imamura, who allowed them to use the facilities at the Institute of Physical and Chemical Research. They acknowledge also Dr. Yoshio Nosaka for his help in the ESR measurement at 4 K.

References and Notes

- (1) (a) Goodman, L. *J. Mol. Spectrosc.* **1961**, *6*, 109–137. (b) Innes, K. K.; Byrne, J. P.; Ross, I. G. *Ibid.* **1967**, *22*, 125–147.
- (2) McGlynn, S. P.; Azumi, T.; Kinoshita, M. "Molecular Spectroscopy of the Triplet State", Prentice-Hall: Englewood Cliffs, N.J., 1969.
- (3) Gerson, F. "High Resolution ESR Spectroscopy", Wiley, New York, 1970.
- (4) Siegbahn, K. In "Handbook of Spectroscopy", Robinson, J. W., Ed.; CRC Press: Cleveland, 1974; Vol. 1.
- (5) (a) Shida, T.; Iwata, S. *J. Phys. Chem.* **1971**, *75*, 2591–2602. (b) *J. Chem. Phys.* **1972**, *56*, 2858–2864. (c) *J. Am. Chem. Soc.* **1973**, *95*, 3473–3483. (d) Shida, T.; Iwata, S.; Imamura, M. *J. Phys. Chem.* **1974**, *78*, 741–749.
- (6) Shida, T.; Nosaka, Y.; Kato, T. *J. Phys. Chem.* **1977**, *81*, 1095–1103.
- (7) Kasai, P. H.; Hedaya, E.; Whipple, E. B. *J. Am. Chem. Soc.* **1969**, *91*, 4364–4368.
- (8) (a) Gleiter, R.; Heilbronner, E.; Hornung, V. *Helv. Chim. Acta* **1972**, *55*, 255–274. (b) Brogli, F.; Heilbronner, E.; Kobayashi, T. *Ibid.* **1972**, *55*, 274–288.
- (9) Hush, N. S.; Cheung, A. S.; Hilton, P. R. *J. Electron Spectrosc. Relat. Phenom.* **1975**, *7*, 385–400.
- (10) Shida, T. *J. Phys. Chem.* **1969**, *73*, 4311–4314.
- (11) Shida, T.; Nosaka, Y.; Kato, T. *J. Phys. Chem.* **1978**, *82*, 695–698.
- (12) Edlund, O.; Lund, A.; Shiotani, M.; Sohma, J.; Thuomas, K. A. *Mol. Phys.* **1976**, *32*, 49–69.
- (13) Hoffmann, R.; Imamura, A.; Hehre, M. J. *J. Am. Chem. Soc.* **1968**, *90*, 1499–1509.
- (14) von Niessen, W.; Diercksen, G. H. F.; Cederbaum, L. S. *Chem. Phys.* **1975**, *10*, 345–360.
- (15) Hinchliffe, A. *J. Electron Spectrosc. Relat. Phenom.* **1977**, *10*, 415–422.
- (16) Scrocco, M.; Lauro, C. D.; Califano, S. *Spectrochim. Acta* **1965**, *21*, 571–577.
- (17) Grimison, A.; Simpson, G. A. *J. Phys. Chem.* **1968**, *72*, 1776–1779.
- (18) Bowers, H. J.; McRae, J. A.; Symons, M. C. R. *J. Chem. Soc. A* **1968**, 2696–2699.
- (19) Nenner, I.; Schulz, G. J. *J. Chem. Phys.* **1975**, *62*, 1747–1758.
- (20) Watanabe, T.; Shida, T.; Iwata, S. *Chem. Phys.* **1976**, *13*, 65–72.
- (21) David, C.; Janssen, P.; Geuskens, G. *Spectrochim. Acta, Part A* **1971**, *27*, 367–376.
- (22) Chaudhuri, J.; Kume, S.; Jagur-Grodzinski, J.; Szarc, M. *J. Am. Chem. Soc.* **1968**, *90*, 6421–6425.

Model Studies of the Electronic Structure of Solid-State Beryllium Borohydride

Dennis S. Marynick

Contribution from the Department of Chemistry, The University of Texas at Arlington, Arlington, Texas 76019. Received May 31, 1979

Abstract: The electronic structure of polymeric solid-state beryllium borohydride is modeled by performing molecular orbital calculations on $(\text{BeB}_2\text{H}_8)_n$ fragments, $n = 1-6$. Comparisons of atomic charges, overlap populations, localized orbitals, and electron density indicate that the solid is best viewed as nearly ionic BeBH_4^+ and BH_4^- ions. This view is consistent with previous crystallographic and infrared work. The convergence of the calculated properties of the molecular wave function as a function of chain length is examined in detail. Fair convergence is observed for $n = 3$, while essentially complete convergence is seen at $n = 5$.

Introduction

Although the structure of beryllium borohydride in the gas phase is a subject of considerable controversy,¹⁻⁵ the solid-phase structure is known with certainty from an X-ray diffraction study.⁶ The solid state consists of one-dimensional helical polymers of alternating boron and beryllium atoms about a 4_1 crystallographic screw axis, with a BH_4 group bound to the outside of the helix at each beryllium site. Figure 1 illustrates the chemical repeat of the polymer, and Figure 2 shows a projection down the helical axis. There is a double hydrogen bridge associated with every near neighbor boron-beryllium interaction, and the hydrogen coordination about beryllium is a distorted trigonal prism. The space group is $I4_1cd$, with unit cell parameters $a = 9.1$ and $b = 13.6$ Å.

Earlier, an infrared study of the solid⁷ was interpreted in terms of the ionic solid $\text{BeBH}_4^+\text{BH}_4^-$. In fact, distances obtained from the X-ray study for $\text{Be}-\text{B}_1$ (1.92 Å), $\text{Be}-\text{B}_2$ (2.00 Å), and $\text{Be}-\text{B}_2'$ (2.00 Å) suggested that the above interpretation may be substantially correct, with B_2 , the boron within the helix, being part of a BH_4^- group and B_1 being part of a BeBH_4^+ group. Nevertheless, the helical polymeric chains

suggest some compromise between the extremes of covalency (the finite molecule) and ionicity (an infinite three-dimensional solid).

In marked contrast to the polymeric nature of the solid state, the gas phase is known^{5a,8} to exist mainly in monomeric units. Many different structures have been suggested,³ but recent electron diffraction^{5b} and infrared^{5a} work tends to favor a two-structure hypothesis, one structure being linear with triple hydrogen bridges, unequal boron-beryllium bond lengths, and C_{3v} symmetry, and the other structure probably being linear with double hydrogen bridges and D_{2d} symmetry. Recent theoretical work^{3,4} is not consistent with the suggested C_{3v} conformer, but suggests that the D_{2d} structure and a linear structure with triple hydrogen bridges and D_{3d} symmetry are competitive energetically. Neither of these structures can account for the observed dipole moment.⁹

In this paper we present a molecular orbital study of models of the solid-state beryllium borohydride polymeric chain, using fragments of from one to six monomeric units and geometrical parameters defined by the previous X-ray diffraction study.⁶ We employ molecular orbital calculations in the approximation of partial retention of diatomic differential overlap